

## Experimental and theoretical investigation of the far-infrared spectrum of H<sub>2</sub>-He mixtures

George Birnbaum

*National Bureau of Standards, Gaithersburg, Maryland 20899*

G. Bachet

*Laboratoire des Interactions Atomiques et Moléculaires, Faculté des Sciences et Techniques de Saint-Jérôme, Marseille 13397, Cedex 4, France*

Lothar Frommhold

*Department of Physics, University of Texas at Austin, Austin, Texas 78712-1081*

(Received 26 March 1987)

New measurements of the rototranslational collision-induced absorption spectra in the far-infrared (FIR) frequency region of gaseous mixtures of hydrogen (H<sub>2</sub>) and helium (He) are reported. The frequency range extends up to 1500 cm<sup>-1</sup> at the temperature of 195 K, and 1700 cm<sup>-1</sup> at 296 K. The uncertainties of the measurement are assessed. Comparison with previous measurements show substantial agreement at frequencies where the measurements overlap. For comparison with the measurement, spectra are computed from the fundamental theory using a state of the art *ab initio* dipole function and an isotropic potential surface as input. The observed agreement suggests that for important applications, such as the analysis of the FIR spectra of the outer planets, the spectra can be obtained reliably as a function of frequency and temperature from quantum calculations of the kind presented here.

### I. INTRODUCTION

Study of the far-infrared (FIR) absorption of H<sub>2</sub>-He mixtures is important for elucidating the nature of collision-induced rototranslational spectra because of the simplicity of the constituents, and the relative simplicity of the spectrum, which consists of several rather well-resolved lines.<sup>1,2</sup> Moreover, since the thermal emission from the major planets is due to pressure-induced absorption in the FIR region resulting from H<sub>2</sub>-He and H<sub>2</sub>-H<sub>2</sub> collisions,<sup>3,4</sup> detailed knowledge of these spectra is needed to interpret this thermal emission in quantitative terms. The first detailed laboratory measurements of the FIR spectrum of H<sub>2</sub>-He mixtures were limited to room temperature in the region from 300 to 1400 cm<sup>-1</sup>.<sup>5,6</sup> About two decades later, these measurements were extended to map the translational band as well as to obtain new data on the hydrogen S<sub>0</sub>(0) and S<sub>0</sub>(1) rotational lines in a study at 77.4, 195, and 292 K in the spectral region from about 20 to 900 cm<sup>-1</sup>.<sup>7</sup> These results were analyzed in terms of a model line shape,<sup>2</sup> and later they were shown to be in good agreement with quantum-mechanical calculations of the spectrum.<sup>8</sup>

This work continues our investigation of the FIR spectrum of H<sub>2</sub>-He by measuring the absorption coefficient of H<sub>2</sub>-He mixtures in the frequency range from 20 to 1700 cm<sup>-1</sup> at 296 K, and from 10 to 1500 cm<sup>-1</sup> at 195 K. The overlap with previous measurements<sup>7</sup> at these temperatures in the range 20 to 900 cm<sup>-1</sup> is important in helping to establish the absolute accuracy of these measurements, which for a variety of reasons are particularly difficult. The new results

beyond 900 cm<sup>-1</sup> make possible a comparison of theory and experiment in the high-frequency wing of this spectrum. From an analysis of the various sources of experimental error, it is suggested that the theoretical results should be more accurate than the experimental results in the H<sub>2</sub>-He system. Consequently, the former are preferable in studies of thermal emission from atmospheres containing H<sub>2</sub> and He.

### II. EXPERIMENTAL ARRANGEMENT

Since the experimental arrangement used here is the same as that employed previously,<sup>9,10</sup> only some brief comments are required. As before, an evacuable monochromator of the Czerny-Turner type, with 15×15-cm<sup>2</sup> gratings, was used generally for frequencies below about 550 cm<sup>-1</sup>. A Perkin Elmer (PE) spectrometer, model No. 112, converted for use with Littrow-mounted gratings, was used generally for frequencies above about 550 cm<sup>-1</sup>. Independent measurements of the absorption coefficient made with each of the monochromators in overlapping frequency ranges generally agreed to better than 5%.

The gas cell was a brass pipe 3.00 m long, with an inner diameter of 12.5 mm, and sealed by high-density polyethylene windows for measurements below 500 cm<sup>-1</sup>, and by thallium bromiodide (KRS-5) windows above 500 cm<sup>-1</sup>. Two H<sub>2</sub>-He mixtures were obtained from Matheson Gas Products (certified grade): 36.8% ultrahigh purity (UHP) H<sub>2</sub>, 63.2% Matheson-grade purity He; 10.6% UHP H<sub>2</sub>, 89.4% Matheson-grade He. According to the Matheson Gas Products catalog for 1985,

these percentages are accurate to 2%. Matheson-purity He contains less than 1 ppm total impurities which include  $N_2$ ,  $O_2$ , Ar,  $CO_2$ , hydrocarbons, and  $H_2O$ . UHP-grade  $H_2$  contains less than 10 ppm total impurities which include CO in addition to the above. Further purification for the reduction of water vapor and other polar impurities such as CO was attempted by passing the gas very slowly through a section of stainless-steel tubing filled with molecular sieve (60/80 screen, type 13X) and immersed in liquid  $N_2$ . The mixture was also passed through sections of stainless-steel tubing containing nickel-silica granular powder as in Ref. 7 where it was used to obtain equilibrium  $H_2$ . Although the difference in the absorption coefficient between normal and equilibrium  $H_2$  at 195 K is of the order of 1%, very much less than the experimental error, this catalyst is also efficient in removing water vapor. Several Heise gauges were used to measure the pressure, and these were used generally in ranges where the error was no more than several tenths of one percent.

The temperature of the bath consisting of dry ice and ethanol, measured by three platinum-resistance thermometers spaced along the bath, was estimated to be known to  $\pm 1$  K. The temperature of the gas cell in air, subject to the ambient temperature of the room was known to within the range  $\pm 2$  K.

### III. EXPERIMENTAL RESULTS

The absorption coefficient  $\alpha(\nu)$  was determined from the relation

$$\alpha(\nu) = L^{-1} \ln[I_0(\nu)/I(\nu)], \quad (1)$$

where  $L$  is the length of the gas cell, and  $I(\nu)$  and  $I_0(\nu)$ , respectively, are proportional to the intensity of the radiation transmitted by the cell filled with the gas under study, and with He at the same pressure. Helium was used to obtain the background  $I_0(\nu)$  to correct for any small change in transmittivity due to distortion of the cell windows by the pressure of the gas. The absorption coefficient per amagat squared,  $\alpha(\nu)/\rho^2$ , determined approximately every  $5 \text{ cm}^{-1}$ , are shown in Figs. 1 and 2. Figure 1 displays the mixture data at 296 K for the 36.8%  $H_2$ -63.2% He mixture, and also shows the contribution due to  $H_2$ - $H_2$  collisions,  $\alpha_{11}x^2$ , and the difference (or enhancement) spectrum due to  $H_2$ -He collisions,  $x(1-x)\alpha_{12}$ ;  $x = \rho_{H_2}/\rho$  is the  $H_2$  concentration and  $\rho$  is the total density. These absorptions at densities where collisions are essentially bimolecular are related by

$$\alpha/\rho^2 = x^2\alpha_{11} + (1-x)\alpha_{12}. \quad (2)$$

The enhancement is obtained by subtracting the  $H_2$ - $H_2$  absorption<sup>9</sup> from that of the mixture.

Measurements of the absorption were also obtained with the 10.6% mixture in the wave number range from about 200 to  $700 \text{ cm}^{-1}$ . The absorption at 195 K for the 10.6% and 36.8% mixtures are shown in Fig. 2. For some unaccountable reason, the data obtained with the 36.8% mixture in the region  $500$ - $600 \text{ cm}^{-1}$  was found

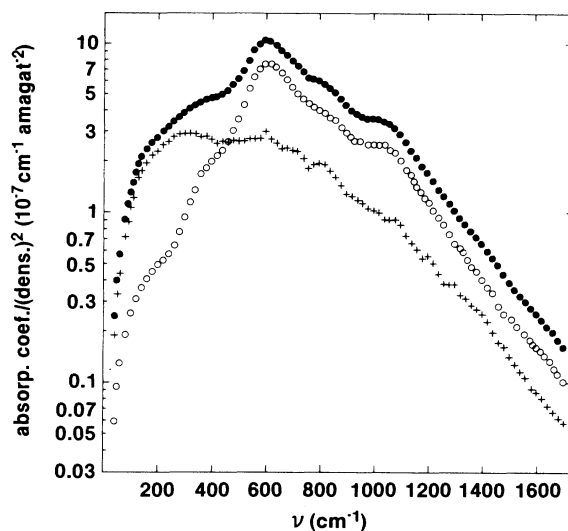


FIG. 1. Far-infrared absorption of a mixture of 36.8%  $H_2$  in He at 296 K. ● is the absorption of the mixture,  $\alpha/\rho^2$ ; ○ is the absorption due to  $H_2$ - $H_2$  collisions,  $\alpha_{11}x^2$ ; + is the absorption due to  $H_2$ -He collisions,  $\alpha_{12}x(1-x)$  [see Eq. (1)].

to be unreliable and are not included in the figure.

The absorption spectra were plotted on a logarithmic scale to display results with an intensity range of several decades, although such plots tend to deemphasize spectral features. The translational band due to  $H_2$ -He collisions makes a significant contribution to the absorption at all frequencies, and the major contribution at frequencies less than roughly  $400 \text{ cm}^{-1}$ . At 296 K (Fig. 1) and 195 K (Fig. 2) in the mixture data, the hydrogen  $S_0(0)$  line ( $354 \text{ cm}^{-1}$ ) is barely discernible as is the  $S_0(2)$  line ( $814 \text{ cm}^{-1}$ ) and the  $S_0(3)$  line ( $1034 \text{ cm}^{-1}$ ). The most prominent feature at both temperatures is the  $S_0(1)$  line

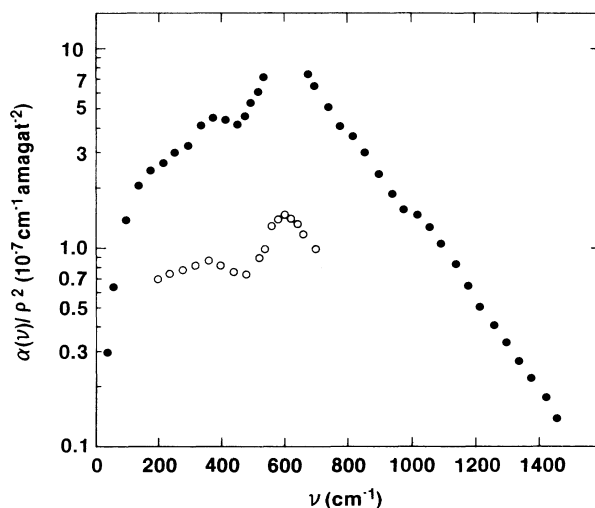


FIG. 2. Absorption at 195 K of 36.8% ● and 10.6% ○ mixtures of  $H_2$  in He. Note all data points are shown.

(587  $\text{cm}^{-1}$ ). The wave number in parentheses is the free rotational frequency; these do not coincide with the apparent positions in the spectrum because of the effect of detailed balance on the band shape. With such broad and rather featureless spectra, spectral slit widths of roughly 10  $\text{cm}^{-1}$  with the low-frequency monochromator, and 2  $\text{cm}^{-1}$  with the high-frequency (PE) monochromator, produced no significant distortion in the recorded spectra.

Table I gives the pressures and densities used in various frequency ranges at 195 and 296 K for the 36.8% and 10.6% mixtures of  $\text{H}_2$  in He. At room temperature, the highest density used was 109 amagats. Since Kiss *et al.*<sup>5</sup> found at this temperature that the integrated absorption per density of  $\text{H}_2$  of the far-infrared band varied linearly with the density of He to 130 amagats, we took our room-temperature absorption as proportional to  $\rho_{\text{H}_2}\rho_{\text{He}}$ . At 195 K, densities in excess of 130 amagats were used at the low and high frequencies. Whereas it has been argued that at frequencies which are high compared to the relevant molecular frequencies a system behaves as if the collisions are binary,<sup>11</sup> this may not be true at the lowest frequencies.<sup>12</sup> Although some tests of the density dependence of the absorption coefficient at some selected frequencies did not reveal any departure from a quadratic density dependence, the accuracy of such tests may not have been sufficient to reveal such an effect, particularly at the lowest and highest frequencies where the absorption coefficient becomes very small.

Independent measurements of  $\alpha(\nu)/\rho^2$  at 296 K of the 36.8% mixture in the frequency region 500–600  $\text{cm}^{-1}$ , where the ranges of the low frequency and PE monochromators overlap, gave results which generally agreed to within 5% or better, but which in some instances diverged by as much as 10%. Determinations of  $\alpha(\nu)/\rho_{\text{H}_2}\rho_{\text{He}}$  with a given monochromator at overlapping grating ranges and at different densities gave results which agreed to within 5% or better, but which in some cases diverged by as much as 10%. The signal-to-noise ratio in measuring  $I$  and  $I_0$  was usually about 1%, and provided the ratio  $I/I_0$  was in the range 0.25–0.75,<sup>13</sup> as was the case except at the very low and high frequencies, the precision in determining  $\alpha(\nu)$  was better than 3%

(see Fig. 4 in Ref. 13). We believe the greater absolute error in measuring  $\alpha(\nu)$  is due to the following effects: window distortion not corrected by measuring  $I_0$  with He, possibly because of hysteresis in the stressing of the windows, some residual gaseous impurity or water vapor which may have entered the system due to some very small leak in the gas handling system, or some undetected drift in the electronics.

The previous discussion deals with the errors in determining the absorption coefficient of a given gas mixture. However, the determination of  $\alpha_{12}$  from Eq. (1) requires the subtraction of two nearly equal contributions in the vicinity of the  $S_0(0)$  and  $S_0(1)$  lines and at the higher frequencies, where the absorption is due mostly to  $\text{H}_2$ - $\text{H}_2$  collisions. Thus small uncertainties in  $\alpha/\rho^2$  and  $\alpha_{11}$  can result in a large fractional error in  $\alpha_{12}$ .<sup>7</sup> We find from Eq. (2) that, when this situation occurs, making  $x$  small by working with a dilute mixture should reduce the fractional error in  $\alpha_{12}$ , although this requires working at higher densities to obtain comparable absorption. In the region from about 200 to 850  $\text{cm}^{-1}$ , where data for the 36.8% and 10.6%  $\text{H}_2$  mixtures were obtained, except for results with the 36.8% in the vicinity of the  $S_0(1)$  line, the rms difference between the absorption coefficients  $\alpha_{12}$  was about 5% at 296 K and 13% at 195 K. Furthermore, the values of  $\alpha_{12}$  obtained with the 36.8% mixture were higher in general than those obtained with the 10.6% mixture.

Bachet<sup>14</sup> has emphasized the need for knowing accurately the concentrations of  $\text{H}_2$  in the mixture. The error in  $\alpha_{12}$  due to an error in the concentration is given by

$$\frac{\Delta\alpha_{12}}{\alpha_{12}} = \frac{-\Delta x}{1-x} \left[ \frac{1-2x}{x} + 2\frac{\alpha_{11}}{\alpha_{12}} \right]. \quad (3)$$

Thus, if we take  $\alpha_{11}/\alpha_{12} \approx 5$  as a representative value in the vicinity of the  $S_0(1)$  line and consider a 35% mixture of  $\text{H}_2$  in He where the concentration of  $\text{H}_2$  is known with accuracy of 2% (which is the accuracy given by Matheson for the mixtures used here), then we obtain  $\Delta\alpha_{12}/\alpha_{12} = 17\%$ . For a 10% mixture and the same values of  $\alpha_{11}/\alpha_{12}$  and  $-\Delta x/x$ , the error in  $\alpha_{12}$  is much less, namely, 4%. At high and, particularly, low fre-

TABLE I. Experimental conditions of temperature, pressure, and density.

$T$ (K)	$\text{H}_2$ (%)	Frequency range ( $\text{cm}^{-1}$ )	Pressure range (psi)	Density range (amagat)
297	36.8	20–90	2000	116
		90–897	1050–810	63–40
		877–1702	1500–1700	89–100
195	10.6	180–864	1845–1600	109–96
	36.8	20–180	2100–1500	175–130
		180–1219	1160–900	103–81
		1220–1590	1825	155
	10.6	180–599	1694–1500	156–38
		500–655	1100	102
660–920		1500	138	

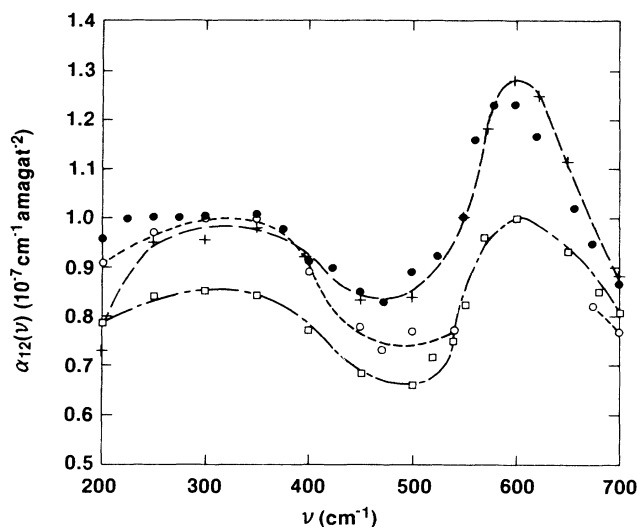


FIG. 3. Comparison of the far-infrared enhanced absorption at 195 K due to H<sub>2</sub>-He collisions. -+-+, Ref. 14; —○—○, present work, 36.8% H<sub>2</sub> in He; —□—□, present work, 10.6% H<sub>2</sub> in He; ●, Ref. 7.

quencies,  $\alpha_{11}/\alpha_{12}$  decreases and so the error in  $\alpha_{12}$  is less.

To help establish the reliability of  $\alpha_{12}$  for H<sub>2</sub>-He, we compared the results of a number of different investigations at 195 K where data in an overlapping frequency range were available. These spectra, which are illustrated in Fig. 3, show excellent agreement between our earlier results<sup>7</sup> and those obtained by Bachet.<sup>14</sup> The results obtained here with the 36.8% mixture also agree well with those just cited. Surprisingly, data obtained with the dilute mixture deviate from the other data by roughly 15%, with greater deviations in certain regions, and shall be excluded from further consideration.

We also compared the 36.8% mixture results at room temperature with the earlier results of Kiss *et al.*<sup>5</sup> In the region 400–1000 cm<sup>-1</sup> the rms difference between these results is an acceptable 12%. In the region from 1100 to 1300 cm<sup>-1</sup>, their highest frequencies, the discrepancy becomes much larger. The reason for this is not clear, but it might be attributable to working with values of transmittance  $I(\nu)/I_0(\nu)$  close to unity, where the fractional error in determining the absorption coefficient becomes very great.<sup>13</sup> As far as we can determine, our transmittance in this region was somewhat smaller. In the comparisons of theory with experiment made later in this paper, one should note that at 195 K the transmittance for the 36.8% mixture was about 0.7 at 1310 cm<sup>-1</sup> and approached unity at the higher frequencies. At 296 K the transmittance was about 0.7 at 1200 cm<sup>-1</sup>, 0.8 at 1300 cm<sup>-1</sup>, and approached unity at the higher frequencies.

#### IV. FUNDAMENTAL THEORY

The rototranslational collision-induced absorption (CIA) spectra can be computed from first principles if

two functions of the intermolecular interaction are known: the induced dipole moment and interaction potential.<sup>15</sup>

##### A. Dipole moment

For the study of the induced dipole moment based on fundamental principles, the collisional H<sub>2</sub>-He complex has been treated elsewhere as a molecule in the self-consistent field (SCF) and size-consistent coupled electron-pair approximations (CEPA).<sup>8</sup> The basis set, which accounts for 95% of the correlation energies, has been shown to separate correctly at distant range. The results have been expressed in terms of spherical harmonics,  $Y_L^m$ , according to

$$\begin{aligned} \mu_M(\mathbf{r}, \mathbf{R}) = & \frac{4\pi}{\sqrt{3}} \sum_{\lambda, L} A_{\lambda L}(r, R) \\ & \times \sum_m C(\lambda, L, 1; m, M-m) Y_{\lambda}^m(\hat{\mathbf{r}}) \\ & \times Y_L^{M-m}(\hat{\mathbf{R}}). \end{aligned} \quad (4)$$

The  $C(\lambda, L, 1; m, n)$  are Clebsch-Gordan coefficients. In this expression,  $\mathbf{r}$  is the vibrational separation of H<sub>2</sub>,  $\mathbf{R}$  connects He with the center of H<sub>2</sub>,  $\hat{\mathbf{r}}$  and  $\hat{\mathbf{R}}$  are the corresponding unit vectors, and  $r$  and  $R$  denote the norms of the vectors. We note that the expansion parameter  $\lambda$  is even and non-negative. The subscript  $M=0, \pm 1$  designates the spherical tensor component of the dipole moment  $\mu$ . For the computation of the spectra, we take the vibrational transition elements of Eq. (4) which defines the expansion coefficients  $B_{\lambda L}(R)$  from the  $r$ -dependent  $A_{\lambda L}(r, R)$ , according to

$$B_{\lambda L}^{vv'}(R) = \langle v | A_{\lambda L}(r, R) | v' \rangle. \quad (5)$$

The dipole components  $\mu_M^{vv'}(\mathbf{R}) = \langle v | \mu_M(\mathbf{r}, \mathbf{R}) | v' \rangle$  are then given by an expression like Eq. (4), with the  $A_{\lambda L}$  replaced by  $B_{\lambda L}^{vv'}$ . For the rototranslational spectra of interest here, we need the average over the vibrational ground state,  $v=v'=0$ . All superscripts  $vv'$  will be dropped from here on.

The four leading  $B_{\lambda L}(R)$  are obtained from the SCF and CEPA calculations at seven separations ( $3 \leq R \leq 10$  bohrs); for these four terms, the values of the expansion parameters are  $\lambda L=01$  (isotropic overlap component),  $\lambda L=21$  (anisotropic overlap component),  $\lambda L=23$  (quadrupole-induced component), and  $\lambda L=45$  (hexadecapole-induced component). At long range, the asymptotic expressions of the quadrupole-induced component agree very closely with the theoretical expression,<sup>16</sup>

$$B_{\lambda L}(R) = \sqrt{\lambda+1} \frac{\alpha(\text{He})Q_{\lambda}(\text{H}_2)}{R^{\lambda+2}}, \quad (6)$$

where  $L=\lambda+1$ , the polarizability of the helium atom is called  $\alpha(\text{He})$ , and the quadrupole strength of hydrogen is  $Q_{\lambda}(\text{H}_2)$ , with  $\lambda=2$ . Even for the hexadecapole-induced component ( $\lambda=4$ ), which amounts to only about 1% of the total induced dipole, the  $B_{45}$  is asymptotically in agreement with Eq. (6). This fact, together with similar

other comparisons, suggests an overall accuracy of the three dominant  $B_{\lambda L}$  components in the order of 2%.<sup>8</sup>

The functions  $B_{\lambda L}$  can be represented in terms of a simple, analytical expression

$$B_{\lambda L}(R) = \frac{B_{\lambda L}^{(n)}}{R^n} + B_{\lambda L}^{(0)} \exp[\alpha_{\lambda L}(R - R_0) + b_{\lambda L}(R - R_0)^2], \quad (7)$$

with  $R_0 = 5.70$  bohrs, i.e., roughly the collision diameter. The values of the constants  $n = n(\lambda L)$ ,  $B_{\lambda L}^{(n)}$ ,  $B_{\lambda L}^{(0)}$ ,  $\alpha_{\lambda L}$ , and  $b_{\lambda L}$  can be found in Table V of Ref. 8.

### B. Potential

The pair interaction potential of the  $H_2$ -He system is among the most thoroughly investigated ones presently known. We choose the *isotropic* part of the *ab initio* surface by Meyer *et al.*,<sup>17</sup> averaged over the ground vibrational state of hydrogen. For the vibrational average, we found the extended tables<sup>18</sup> useful; third-order spline interpolation of the numerical tables is employed for accuracy.

### C. The spectra

With the dipole function and potential described, we compute the rototranslational spectra from first principles, using the quantum formalism described elsewhere<sup>15,19</sup> at the temperatures of the measurements discussed above. For easy comparison with a previous measurement,<sup>7</sup> a spectrum at 292.4 K is also calculated which differs by more than 3% from the 297-K spectrum only at high frequencies ( $> 1100 \text{ cm}^{-1}$ ). Since the isotropic interaction potential does not support bound states and "sharp" scattering resonances, the line-shape computations are straightforward. Convergence is obtained by summing over 33 partial waves of the initial state. For every one of the four  $\lambda L$  values, translational profiles,  $g_{\lambda L}(\omega; T)$ , are obtained from Eq. (22) of Ref. 15 at 15 frequencies (namely, 3, 8, 20, 40, 70, 100, 140, 200, 280, 360, 450, 560, 680, 800, and  $1000 \text{ cm}^{-1}$ ). The red wings (at negative frequencies) are obtained from the principle of detailed balance [Eq. (27) of Ref. 15] from the intensities of the blue wing. The integration over the initial-state energies of the squared dipole matrix elements is based on 22 energies ranging from about  $kT/20$  to  $12kT$ ;  $k$  is the Boltzmann constant. The rototranslational collision-induced spectra are then constructed by superposition of the appropriately shifted translational profiles, according to Eqs. (21) and (24) of Ref. 15. By suitable variations of the grid widths, etc., the numerical uncertainty of the line-shape computations was estimated not to exceed 1%; in the far wings, for frequency shifts greater than  $1000 \text{ cm}^{-1}$ ; slightly greater uncertainties are possible ( $\approx 2\%$ ).

In order to test the results of the line-shape computations, we have computed the lowest three spectral moments of the translational profiles with their sum rules.<sup>20</sup> These have been evaluated from the potential and dipole functions directly, using an exact quantum formalism de-

scribed elsewhere.<sup>21</sup> Such sum-rule computations can be made with a numerical precision of better than 0.6%. For the calculation of spectral moments from the computed profiles, it is necessary to extend the spectrum to frequencies higher than that shown in Figs. 4 and 5, particularly for the evaluation of the second moment. This high-frequency wing is obtained by simple extrapolation to high frequencies in a semilogarithmic grid. For the zeroth moments, the extrapolation does not affect the numerical precision discernibly. For the first moment, extrapolations introduced marginally significant errors ( $\sim 1\%$ ), but for the second moments up to 10% uncertainty may result for some profiles. Apart from these understandable circumstances, the comparison of the spectral moments and evaluated sum formulas indicates a numerical precision of the line-shape computations of about 1%, in agreement with the above estimate.

Computed spectra are compared with the most reliable measurements in Figs. 4 and 5. At the low frequencies ( $< 800 \text{ cm}^{-1}$ ), Birnbaum's earlier measurements are shown;<sup>7</sup> only a few selected points of the new measurements are here displayed at the low frequencies. In Fig. 4 the low-frequency part is computed for the temperature of 292.4 K. At frequencies higher than  $1100 \text{ cm}^{-1}$ , where the 297 K computation differs by more than 3% from the 292 K results, the 297 K data are shown. The early data<sup>7</sup> in Figs. 4 and 5 to about  $800 \text{ cm}^{-1}$  agree reasonably well with the data obtained here in the overlapping frequency regime. The recent results of Bachet<sup>14</sup> at 195 K are in even closer agreement with Birnbaum's earlier results<sup>7</sup> (see Fig. 3).

The agreement of the measurements with the fundamental theory is generally very satisfactory. At the higher temperature, Fig. 4, the new measurement is in very good agreement with theory, except at frequencies from about 1300 to  $1500 \text{ cm}^{-1}$  where the measurement is greater than theory by a maximum of 20%. At the lower temperature, Fig. 5, the new measurement is consistently above theory by 15%–25% at frequencies higher than  $1000 \text{ cm}^{-1}$ ; the agreement at the lower frequencies is within several percent, better than expected.

### D. The effect of the anisotropy of the interaction

The theoretical line shapes displayed in Figs. 4 and 5 were obtained in the isotropic potential approximation. Although the anisotropy of the hydrogen molecule is known to be quite small, it is of interest to estimate the effects of the anisotropy on the CIA spectra in quantitative terms where possible. The anisotropy of the intermolecular interaction has recently been accounted for in exact line-shape calculations.<sup>22</sup> However, close-coupling computations of that kind are very expensive and have been made available only at low temperatures. Nevertheless, recent studies<sup>23,24</sup> of the effect of the anisotropy on spectral moments have indicated what effect the anisotropy has on the spectra. We note that the *ab initio* potential surface<sup>17</sup> provides the currently most dependable information of the anisotropy of the  $H_2$ -He system.

At the temperatures of interest, the intensities of the main hydrogen  $S_0$  lines are insignificantly reduced when the anisotropy is accounted for.<sup>23,24</sup> At the same time,

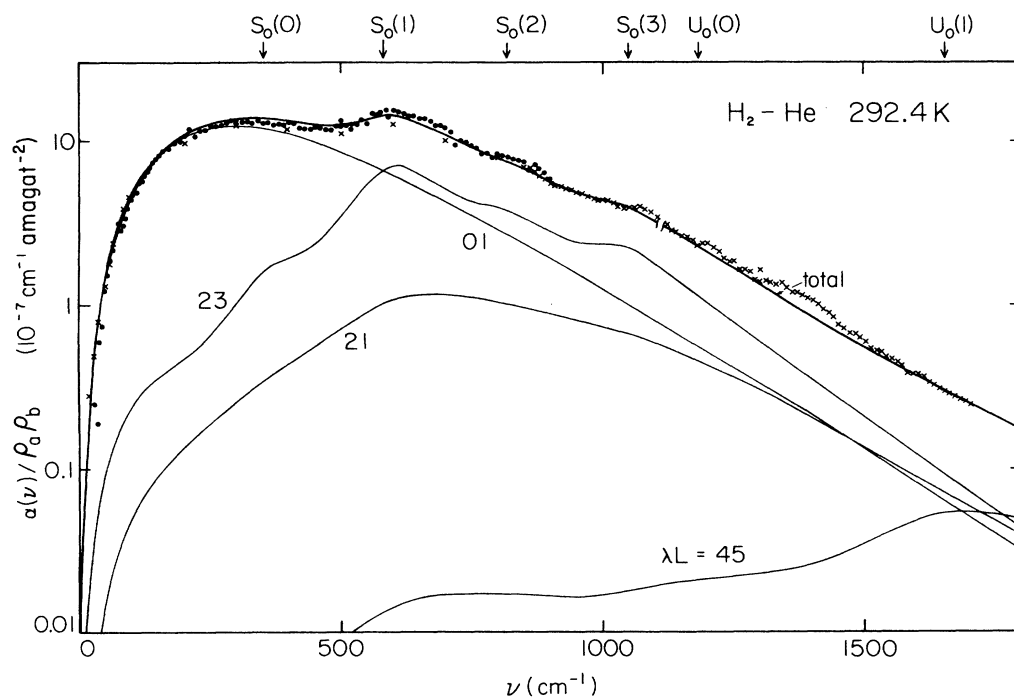


FIG. 4. Absorption of the four significant dipole components, labeled  $\lambda L=01, 21, 23, 45$ , and their sum (marked "total"), according to the fundamental theory, at the temperature of 292.4 K for frequencies from 0 to 1100  $\text{cm}^{-1}$ , and 297 K above 1100  $\text{cm}^{-1}$ . ●, measurement of Ref. 7; ×, present measurement.

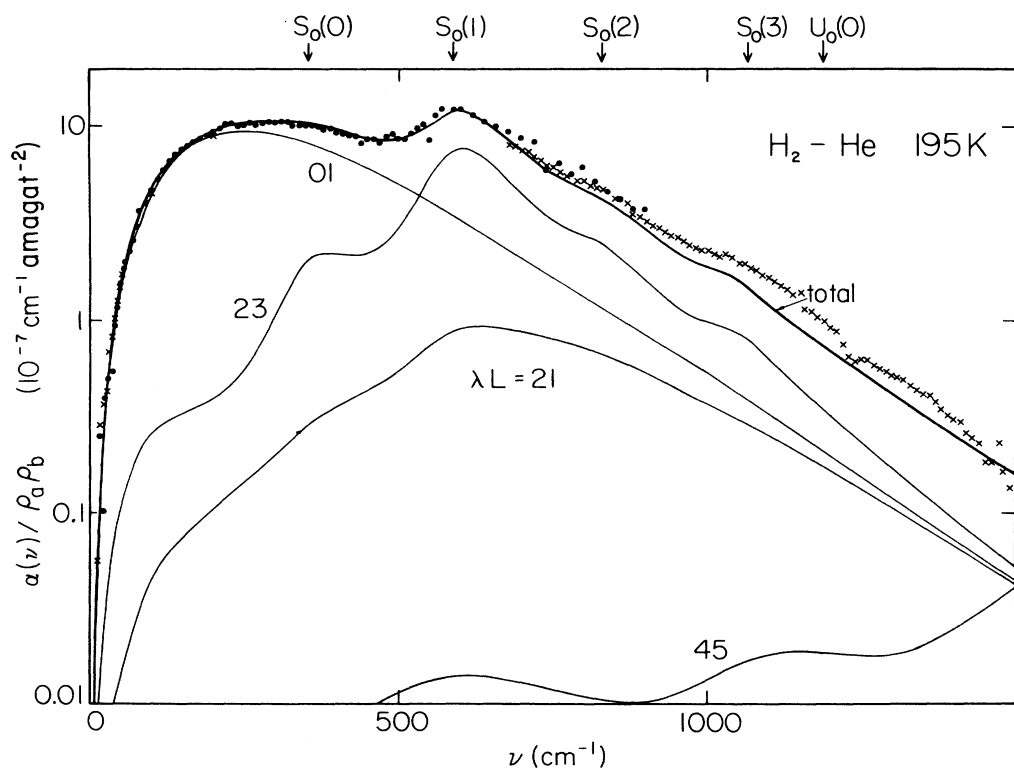


FIG. 5. Absorption of the four significant dipole components, labeled  $\lambda L=01, 21, 23, 45$ , and their sum (marked "total"), according to the fundamental theory, at the temperature of 195 K. ●, measurement of Ref. 7; ×, present measurement.

their widths become slightly greater. However, the intensities of the weak lines, most notably the  $U_0(J)$  lines (which have not yet been resolved in the far-infrared  $H_2$ -He spectrum), are increased by the anisotropy by amounts in the order of 100%. This enhancement arises from the coupling of the various dipole components by the anisotropy of the interaction. In other words, near the centers of the main  $S_0$  lines, the anisotropy will be nearly without an effect. In the far wing ( $> 1000 \text{ cm}^{-1}$ ), however, the broadening of mainly the  $S_0(1)$  line may increase the wing intensities somewhat. Furthermore, the weak  $U_0(1)$  and  $U_0(2)$  lines will be strengthened which leads to a further feeble increase in the far wing. These two enhancements arising from the anisotropy should be stronger at the higher temperature.<sup>23,24</sup>

The measurements deviate more strongly from the (isotropic) theory at the lower temperature (Fig. 5). Furthermore, the observed excess intensity from about 1300 to 1500  $\text{cm}^{-1}$  at 297 K does not really coincide with an  $U_0(J)$  line of hydrogen. We conclude that the observed small deviations of the far wing of the measurements from the theory is quite likely noise in this region of very small absorption.

#### V. CONCLUSION

New determinations of the far wings of the roto-translational CIA spectra of  $H_2$ -He have been obtained up to frequencies around 1700  $\text{cm}^{-1}$  from laboratory measurements. These are compared with a quantum line-shape computation based on the fundamental theory. The agreement is very good at frequencies from roughly 0 to 1000  $\text{cm}^{-1}$ . However, at some of the higher frequencies, especially at the lower temperature, deviations between 15% and 25% are observed. A discussion of the rather feeble effects of the anisotropy of the intermolecular interaction, which were neglected in the line-shape computation, appear to rule out these

effects as the reason for the above deviations. We suggest that the observed deviations at low temperature are due to an increased uncertainty of the measurements arising from the smallness of the absorption. An error estimate of the measurement is consistent with an uncertainty of this order.

The type of agreement observed here between the spectroscopic measurements and the line-shape computations based on the fundamental theory is unusual, if not unique in the field of the collision-induced spectroscopies. The most advanced SCF and CEPA calculations of the induced dipole function, when combined with an exact quantum line-shape formalism and a proven interaction potential, permit the computation of such spectra with an accuracy which matches or exceeds that of even the best spectroscopic measurements. This fact is significant in situations where such spectra need to be known accurately at a variety of temperatures. For the modeling of the atmospheres of the distant planets, for example, temperatures down to about 40 K are important, and for the late stars and white dwarfs, temperatures of several thousand K must be considered, which pose severe problems in precision laboratory measurements. Theory, on the other hand, has no such limitations and should provide reliable spectra under almost any conditions, at least for the light molecular systems involving hydrogen.

#### ACKNOWLEDGMENTS

The authors thank Dr. P. Dore and Dr. H. Sutter for assistance with the measurements. The work performed at the University of Texas was supported by the National Science Foundation Grant No. AST-8613085. The work performed at the National Bureau of Standards was supported by a contract from the Jet Propulsion Laboratory, sponsored by the Planetary Atmospheres Program of NASA.

- <sup>1</sup>H. L. Welsh, in *Spectroscopy*, Vol. III of *MTP Int. Rev. of Science—Physical Chemistry*, edited by D. A. Ramsey (Butterworths, London, 1972), pp. 33-71.
- <sup>2</sup>E. R. Cohen, L. Frommhold, and G. Birnbaum, *J. Chem. Phys.* **77**, 4933 (1982); **78**, 5283(E) (1983).
- <sup>3</sup>L. M. Trafton, *Astrophys. J.* **179**, 971 (1973).
- <sup>4</sup>G. S. Orton and A. P. Ingersoll, in *Jupiter*, edited by I. Gehrels (University of Arizona, Tucson, 1976), p. 207.
- <sup>5</sup>Z. J. Kiss, H. P. Gush, and H. L. Welsh, *Can. J. Phys.* **37**, 362 (1959).
- <sup>6</sup>Z. J. Kiss and H. L. Welsh, *Can. J. Phys.* **37**, 1249 (1959).
- <sup>7</sup>G. Birnbaum, *J. Quant. Spectrosc. Radiat. Transfer* **19**, 51 (1978). [The following error was noted in Eq. (3). The factor  $8/\theta_m^2$  should be inverted, and  $\theta_m = 1/2f$ .]
- <sup>8</sup>W. Meyer and L. Frommhold, *Phys. Rev.* **34**, 2771 (1986).
- <sup>9</sup>G. Bachet, E. R. Cohen, P. Dore, and G. Birnbaum, *Can. J. Phys.* **61**, 591 (1983).
- <sup>10</sup>G. Birnbaum, A. Borysow, and H. G. Sutter (to be published).
- <sup>11</sup>D. W. Oxtoby, *Molec. Phys.* **34**, 987 (1977).
- <sup>12</sup>J. D. Poll, in *Intermolecular Spectroscopy and Dynamical Properties of Dense Systems*, Proceedings of the International School of Physics "Enrico Fermi," Course LXXV, Varenna,

- 1978, edited by J. van Kranendonk (North-Holland, Amsterdam, 1980), pp. 45-76.
- <sup>13</sup>I. F. Silvera and G. Birnbaum, *Appl. Opt.* **9**, 617 (1970).
- <sup>14</sup>G. Bachet (unpublished).
- <sup>15</sup>G. Birnbaum, Shih-I Chu, A. Dalgarno, L. Frommhold, and E. L. Wright, *Phys. Rev. A* **29**, 595 (1984).
- <sup>16</sup>J. D. Poll and J. L. Hunt, *Can. Phys.* **54**, 461 (1976).
- <sup>17</sup>W. Meyer, P. C. Hariharan, and W. Kutzelnigg, *J. Chem. Phys.* **73**, 1880 (1980).
- <sup>18</sup>J. Schäfer and W. E. Köhler, *Phys. Status Solidi A* **129**, 469 (1985).
- <sup>19</sup>J. Borysow and L. Frommhold, in *Phenomena Induced by Intermolecular Interactions*, edited by G. Birnbaum (Plenum, New York, 1985), p. 67.
- <sup>20</sup>J. D. Poll and J. van Kranendonk, *Can. J. Phys.* **39**, 189 (1961).
- <sup>21</sup>M. Moraldi, A. Borysow, and L. Frommhold, *Chem. Phys.* **86**, 339 (1984).
- <sup>22</sup>J. Schäfer (private communication).
- <sup>23</sup>M. Moraldi, A. Borysow, J. Borysow, and L. Frommhold, *Phys. Rev. A* **34**, 632 (1986).
- <sup>24</sup>M. Moraldi, A. Borysow, and L. Frommhold, *Phys. Rev. A* **36**, 3679 (1987).